An adaptive pre-signal setting to provide bus priority under a coordinated traffic-responsive network

Yi Zhang

Abstract— **The transits constitute the traffic skeleton of the city. With the installation of the high-tech sensors and the emergence of the high-speed communication, interest to grant bus priority via traffic signals grows rapidly during recent years. Pre-signal is an additional traffic signal located upstream of the main signal, which is used to discontinue the private cars and accordingly allow buses jumping the car queue. Compared with the traditional dedicated bus lane through the whole link, the pre-signal can provide bus priority meanwhile minimizing the negative impacts on car traffic. In this paper, we propose an adaptive signal strategy for a traffic network by adjusting the pre-signal as well as the main signal in order to minimize the total passenger delay. A macroscopic model based on cell transmission model is developed, where the link is partitioned into the car cell, the bus cell and the mixed cell. The merging and the diverging of the car flow and the bus flow are elaborated modeled for each type of the cell. With the aim to obtain the signal setting in real time, the harmony search algorithm is adopted to solve the optimization problem. Finally, the case studies illustrate the efficacy of the proposed strategy.**

Index Terms – bus movement management, dedicated bus lane, adaptive pre-signal setting, harmony search algorithm

I. INTRODUCTION

Transit services are undoubtedly effective solutions to tackle the traffic congestion in modern urban cities due to its large ridership, lower resource consumption and environmental-friendly characteristics. Therefore, many studies have been proposed and implemented to improve the traffic performance of transit vehicles, which leads to a positive cycle that more passengers are attracted to select public transits and the usage of private cars is consequently reduced.

Transit signal priority (TSP) control, as a commonly used strategy to provide bus priority, facilitates the bus movement by adjusting the intersection signal to get buses through the intersection without stopping by red signals [11]. Many conditional priority strategies are proposed with the aim to provide bus priority to minimize the schedule deviation but also reduce the additional delay bringing to other traffic users. Ma et al. propose a model-based signal control strategy by extending green time or early terminating red time to smooth bus movement through the corridor [12]. A multi-modal traffic signal strategy is presented by combining a mixed-integer linear programming (MILP) model with the actuated signal control, where a constraint involving virtual requests is developed in MILP to enhance the signal coordination [7]. Hu et al. design a coordinated transit signal priority approach by presenting a MILP model incorporating the green re-allocation strategy instead of traditional strategies called ”green extension” and ”red truncation” [8], which is later extended to consider multiple requests in [9]. Although many strategies are proposed in TSP, its inevitable disadvantage is that the provided priority would definitely increases the delay of private cars in other directions, and the additional received green time may increase the potential possibility of the congestion at the downstream link [11].

Beside the TSP control, dedicated bus lane (DBL) is also a typical approach to provide bus priority. However, DBL occupies a complete lane, which may cannot be provided in some urban areas due to the insufficient road space. Also, the setting of DBL reduces the link capacity and it becomes redundant especially when bus frequency is low [3]. In view of this, intermittent bus lane (IBL) is accordingly raised in order to increase the link discharging flow. Viegas and Lu firstly introduce the concept of IBL, which is defined as a lane whose status changes according to the presence of the bus: the lane changes to DBL if a bus is driving on the lane, otherwise, it opens to other traffics [14]. After that, the IBL is theoretically analyzed in [1], which indicates that the IBL does not significantly reduce the link capacity but is not recommended when the link is near the capacity.

Another approach to provide bus priority is the pre-signal setting. It does not take a whole lane away from private cars like DBL and also does not change the lane status like IBL, which may confuse drivers and leads to corresponding safety issues. Pre-signal is a traffic signal located upstream of the main signal to either provide bus priority to allow bus to jump car queues or relocate the traffic queue without additional road construction to increase link discharging rate [15][16]. When a link, formed by a dedicated bus lane and other normal traffic lanes, sets a pre-signal upstream of the main signal to provide the bus priority, all lanes are used to discharge car traffics after the pre-signal if no bus is coming, otherwise, the pre-signal will change to red for cars to release buses [2]. The impacts of the pre-signal was firstly analysed in [15], however, the settings of the pre-signal and the main signal are all fixed, which is extended and analytically investigated in [2] and [3], where an offset between the pre-signal and the main signal is considered in order to let buses jump car queues when the main signal is red and minimize the car delay as much as possible, also, the pre-signal will change to red once the bus is approaching and change back to green when it passes. And this strategy is implemented in VISSIM, a commercial traffic simulator, and validated via field data to further investigate the impacts it brings to buses and private cars [5]. After that, Guler et al. found that the application domain of the pre-signal depends on three major factors: saturation degree, bus frequency and bus occupancy [4]. Based on the three factors, an adaptive pre-signal setting

Yi Zhang is affiliated with with the Institute for Infocomm Research (I2R), Agency for Science, Technology and Research (A*STAR), Singapore 138632. Emails: zhang_yi@i2r.a-star.edu.sg.

is proposed with the aim to smooth bus movement as well as reduce the influence on the car side [6]. Moreover, a pre-signal control strategy is presented in [10] from the optimal control perspective, however, the model is continuous and not realistic to be implemented in the real world. Although many studies have been conducted on the pre-signal, few studies discuss the adaptive tuning on both pre-signal and the main signals, also, studies develop the model for an isolated intersection under the queuing theory without considering the coordinated one. Therefore, this paper is proposed to fill the gap.

This paper proposes an adaptive signal strategy for the pre-signal as well as the main signal, Adaptive Main Signal with Adaptive Pre-signal (AMAP), with the aim to minimize the total passenger delay for a connected urban traffic network. The paper is organized as follows. The descriptions of the flow-based model are presented in Section II. Simulation results are described in Section III. Conclusions are drawn in Section IV.

II. Formulation of a Network-Based Bus-Car Mixed-Flow Model

A. Problem statement

The road network in the paper is defined as a directed graph $\mathcal{G} = \{\mathcal{J}, \mathcal{L}\}$, where $\mathcal{J}$ is the set of junctions, and $\mathcal{L}$ is the link between two adjacent junctions, which is drawn in Fig. 1. Also, the dedicated bus lanes and the normal car lanes are all existed in the road network, which are denoted as $\mathcal{L}^b$ and $\mathcal{L}^c$, respectively, and we have $\mathcal{L}^b, \mathcal{L}^c \subseteq \mathcal{L}$. As a coordinated network is considered in the system, CTM, one of the macroscopic model, is adopted here to capture the vehicle flow characteristics on the one hand and guarantee a real-time control under a network-based large problem scale on the other hand.

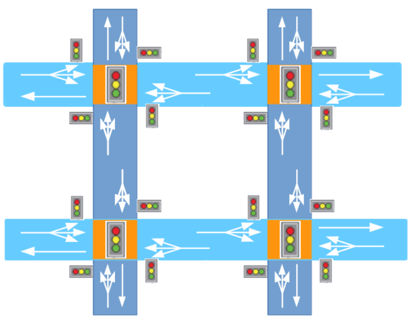

Fig. 1: Layout of the network with pre-signals and main signals

Two levels of control is considered in the system: the main signal in each intersection and the pre-signal upstream of the main signal. The link is partitioned into three types of cells: the bus cell, the car cell and the mixed cell, are highlighted in red, blue and yellow in Fig. 2, respectively. Fig. 2 only draws one lane for each type of vehicles, and it can be multiple lanes when the specific background is involved, which is also a variable in our model.

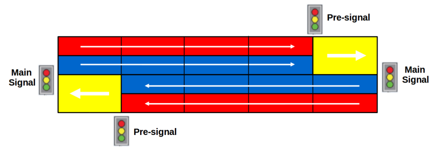

Fig. 2: Layout of the link with pre-signals and main signals

B. Model Description

The bus cell and the car cell only involve buses and other cars, respectively. While both buses and cars can driving on any lanes of the mixed cell.

1) Volume dynamics in each bus cell: The update of the volume of bus cell j is determined by the incoming bus flow $\sum_i f_{ij}^b(k)$ and the outgoing bus flow $\sum_q f_{jq}^b(k)$:

$$\begin{aligned}&(\forall i \in \mathcal{C}_j^b, q \in \mathcal{O}_j^b)\\ &C_j^b(k+1) = C_j^b(k) + \sum_i f_{ij}^b(k) - \sum_q f_{jq}^b(k)\end{aligned} \tag{1}$$

where i, j and q are the index of the cell, $\mathcal{C}_j^b$ is the set of upstream cells providing incoming bus flows for cell j, and $\mathcal{O}_j^b$ is the set of downstream cells receiving outgoing bus flows from cell j. $C_j^b(k)$ represents the number of buses in the cell j at k. $f_{ij}^b(k)$ is the bus flow from cell i to cell j during k.

2) Volume dynamics in each car cell: The update of the volume of car cell j is determined by the incoming car flow $\sum_i f_{ij}^c(k)$ and the outgoing bus flow $\sum_q f_{jq}^c(k)$:

$$\begin{aligned}&(\forall i \in \mathcal{C}_j^c, q \in \mathcal{O}_j^c)\\ &C_j^c(k+1) = C_j^c(k) + \sum_i f_{ij}^c(k) - \sum_q f_{jq}^c(k)\end{aligned} \tag{2}$$

where $\mathcal{C}_j^c$ is the set of upstream cells providing incoming car flows for cell j, and $\mathcal{O}_j^c$ is the set of downstream cells receiving incoming car flows from cell j. $C_j^c(k)$ represents the number of cars in the cell j at k. $f_{ij}^c(k)$ is the car flow from cell i to cell j during k.

3) Volume dynamics in each mixed cell: The update of the volume in mixed cell j is determined by the incoming&outgoing car flow $\sum_r f_{rj}^c(k)$, $\sum_q f_{jq}^c(k)$ and the incoming&outgoing bus flow $\sum_i f_{ij}^b(k)$,$\sum_p f_{jp}^b(k)$:

$$\begin{aligned}&(\forall r \in \mathcal{C}_j^c, q \in \mathcal{O}_j^c, i \in \mathcal{C}_j^b, p \in \mathcal{O}_j^b)\\ &C_j^m(k+1) = C_j^m(k) + \sum_r f_{rj}^c(k) + \sum_i f_{ij}^b(k)\\ &- \sum_q f_{jq}^c(k) - \sum_p f_{jp}^b(k)\end{aligned} \tag{3a}$$

$$C_j^m(k) = C_j^b(k) + C_j^c(k) \tag{3b}$$

where r is also the index of the cell, and $C_j^m(k)$ represents the total number of cars and buses in the mixed cell j at k.

4) Bus flow constraints: The bus flow $f_{ij}^b(k)$ is different according to the type of the cell it comes from: (1) If the bus flow is from the bus cell which is not the one just in front of the pre-signal, then the bus flow is determined by the current cell volume $C_i^b(k)$, the saturation flow rate $\lambda^b k^* v^* \triangle$ and the remaining space of the downstream bus cell $Cap_b - C_j^b(k)$.

(2) If the bus flow is from the bus cell just in front of the pre-signal, then the bus flow is determined by the current cell volume $C_i^b(k)$, the saturation flow rate $\lambda^b k^* v^* \triangle$ and the remaining space of the downstream mixed cell $\lfloor \frac{1}{\beta}(Cap_m - C_j^c(k) - \beta C_j^b(k)) \rfloor$. (3) If the bus flow is from the mixed cell, then it is determined by the bus demand in current mixed cell under turning ratio $\alpha_{ij}^b(k)$, $\alpha_{ij}^b(k) C_i^b(k)$, the saturation flow rate of the mixed cell $(\lambda^b + \lambda^c) k^* v^* \triangle$ and the remaining space of the downstream bus cell $Cap_b - C_j^b(k)$ which is located in another link.

$$f_{ij}^b(k) = \begin{cases} \min\{C_i^b(k), \lambda^b k^* v^* \triangle, Cap_b - C_j^b(k)\} \\ \qquad\qquad\qquad\qquad \text{if} \quad i \in (\mathcal{E}^b \backslash \mathcal{E}_p^b) \\ \min\{C_i^b(k), \lambda^b k^* v^* \triangle, \\ \lfloor \frac{1}{\beta}(Cap_m - C_j^c(k) - \beta C_j^b(k)) \rfloor\} \ \text{if} \quad i \in \mathcal{E}_p^b \\ \min\{\alpha_{ij}^b(k) C_i^b(k), (\lambda^b + \lambda^c) k^* v^* \triangle, \\ Cap_b - C_j^b(k)\} \qquad\qquad \text{if} \quad i \in \mathcal{E}^m \end{cases} \tag{4a}$$

where $\triangle$ is the time interval between k and $k+1$, and Cap_b is the capacity of the bus cell, while Cap_m is the maximum number of cars that cell m can accommodate. $\mathcal{E}^b$ and $\mathcal{E}^m$ are the set of bus cells and the set of mixed cells, respectively. $\mathcal{E}_p^b$ is the set of bus cells just upstream the pre-signal. β is the parameter to transform bus to the equivalent car. $\alpha_{ij}^b(k)$ denotes the turning ratio of buses from link i to link j. λ^b and λ^c are the number of bus lanes and the number of car lanes, respectively. k^* and v^* are the critical density and the critical speed, respectively, and its multiplication determines the saturated flow rate. By transforming the bus volume to corresponding car volume, $Cap_m - C_j^c(k) - \beta C_j^b(k)$ denotes the remaining number of cars that cell j can accommodate.

5) Car flow constraints: The car flow $f_{ij}^c(k)$ is also different according to the type of the cell it comes from: (1) If the car flow is from the car cell which is not the one just in front of the pre-signal, then the car flow is determined by the current cell volume $C_i^c(k)$, the saturation flow rate $\lambda^c k^* v^* \triangle$ and the remaining space of the downstream car cell $Cap_c - C_j^c(k)$. (2) If the car flow is from the car cell just in front of the pre-signal, then the car flow is determined by the current cell volume $C_i^c(k)$, the saturation flow rate $\lambda^c k^* v^* \triangle$ and the remaining space of the downstream mixed cell $Cap_m - C_j^c(k) - \lfloor \beta C_j^b(k) \rfloor$. (3) If the car flow is from the mixed cell, then it is determined by the car demand in current mixed cell under turning ratio $\alpha_{ij}^c(k)$, $\alpha_{ij}^c(k) C_i^c(k)$, the saturation flow rate of the mixed cell $(\lambda^b + \lambda^c) k^* v^* \triangle$ and the remaining space of the downstream car cell $Cap_c - C_j^c(k)$ which is located in another link.

$$f_{ij}^c(k) = \begin{cases} \min\{C_i^c(k), \lambda^c k^* v^* \triangle, Cap_c - C_j^c(k)\} \\ \qquad\qquad\qquad\qquad \text{if} \quad i \in (\mathcal{E}^c \backslash \mathcal{E}_p^c) \\ \min\{C_i^c(k), \lambda^c k^* v^* \triangle, \\ Cap_m - C_j^c(k) - \lfloor \beta C_j^b(k) \rfloor\} \quad \text{if} \quad i \in \mathcal{E}_p^c \\ \min\{\alpha_{ij}^c(k) C_i^c(k), (\lambda^b + \lambda^c) k^* v^* \triangle, \\ Cap_c - C_j^c(k)\} \qquad\qquad \text{if} \quad i \in \mathcal{E}^m \end{cases} \tag{5a}$$

where Cap_c is the capacity of the car cell, and $\mathcal{E}^c$ is the set of car cells. $\mathcal{E}_p^c$ is the set of car cells just upstream the pre-signal. $\alpha_{ij}^c(k)$ denotes the turning ratio of cars from link i to link j.

6) Main signal logic: The main signal at the intersection controls the right of way of traffic flows, under our discrete-time model, only one phase can be activated at each time interval, as shown in equation (6a). Constraint (6b) indicates that the flows, buses and cars, under the same phase must be 0 if the traffic light state for this phase is red. Also, constraint (6c) restricts that the duration of each phase cannot less than the minimum green duration.

$$\sum_{o \in \Omega^J} \theta_o^J(k) = 1 \tag{6a}$$

$$(\forall i \in \mathcal{E}^m)((i,j) \in \mathcal{F}_o^J)$$
$$\theta_o^J(k) = 0 \rightarrow f_{ij}^{c/b}(k) = 0 \tag{6b}$$

$$\theta_o^J(k) = 0 \wedge \theta_o^J(k+1) = 1 \rightarrow$$
$$\prod_{i=1}^{\lfloor \frac{G_{min}}{\triangle} \rfloor} \theta_o^J(k+i) = 1 \tag{6c}$$

where Ω^J is the set of phases in intersection J with each phase $o \in \Omega^J$, and $\mathcal{F}_o^J$ denotes the set of flows passing intersection J under phase o. $\theta_o^J(k)$ is a binary variable, which denotes the state of phase o for the main signal at k. If it is equal to 1, phase o is activated and corresponding compatible flows obtain green, otherwise, the signal state is red. G_{min} is the minimum green duration for each phase.

7) Pre-signal logic: If the pre-signal changes to red, the corresponding car flow should be 0, which makes it possible for buses to jump car queues.

$$(\forall i \in \mathcal{E}_p^c) \quad \theta_l^p(k) = 0 \rightarrow f_{ij}^c(k) = 0 \tag{7}$$

where $\theta_l^p(k)$ is a binary variable, which denotes the state of the pre-signal in link l at k. If it is equal to 0, the signal changes to red, accordingly, cars are blocked and the priority is provided to buses, otherwise, the pre-signal is green.

C. Cost Function

In order to minimize the total passenger delay, the cost is formulated as follows:

$$J = \min \sum_k \sum_i [W_c(C_i^c(k) - f_{ij}^c(k)) + W_b(C_i^b(k) - f_{ij}^b(k))] \triangle \tag{8}$$

where W_c and W_b are the average number of passengers for each private car and each bus, respectively.

The flow equations in the model are formulated by piece-wise functions, which requires to introduce many additional variables to transform into associated linear constraints. Therefore, it is tedious to transform our problem into a MILP problem and is also time-consuming to solve a MILP problem with many variables especially when the problem scale is large. In view of this, the harmony search (HS) algorithm, one of the evolutionary algorithm, is adopted here to solve our problem due to its high performance on many traffic problems [18][17][19], although the optimal result cannot be guaranteed, a good result in real time is more necessary from the application perspective.

III. Simulation Results

In this section, we test the proposed algorithm, AMAP, under several different cars' arrival rates, bus occupancies and bus headways on a three-intersection corridor, as shown in Fig. 3. The strategy with only Adaptive Main signal (AM), the traditional Fixed Main signal strategy with the Fixed Pre-signal setting (FMFP) and the traditional Fixed Main signal strategy without pre-signal setting (FM) are also applied on the studied corridor, and the comparison between the proposed algorithm and the other three methods are analyzed to investigate the efficiency of the proposed method.

The corridor in the case study has 3 intersections and 10 links, and two bus lines are located at the arterial approaches from left to right and from right to left, respectively. Accordingly, 6 pre-signals are set in front of the 3 main signals for two bus lines under opposite directions. The average car arrival flow rates are listed for the column links, which is shown in Fig. 3. The arrival flow rate for two arterial approaches, A_{LR} and A_{RL}, are listed in Table I according to the different congestion levels. Also, each main link (row links in Fig. 3) involves two bidirectional car lanes and two bidirectional bus lanes, and only two car lanes with opposite directions are considered for each minor link (column links in Fig. 3). Two phases drawn in Fig. 4 are discussed in the experiments, and the turning flows involving more phases will be further studied in our future work.

Table II enumerates 12 test cases under the low car arrival rate for main links, various bus occupancies and bus headways. The low car arrival rate for the test cases is 1080 veh/h, which is also listed in Table I. The ratio between the car arrival rate and the saturation flow rate is used to represent the corresponding congestion level. Three different bus occupancies, 30, 80 and 160, and four bus headways, 1 min, 3 min, 6 min and 9 min, are selected in the simulation. For cases 13 to 24 and cases 25 to 36, their bus occupancy and the bus headway are the same as the cases 1 to 12, the only difference is that cases 13 to 24 and cases 25 to 36 correspond to the medium car arrival flow rate ($\frac{A_{LR/RL}}{S} = 1.0$) and the high car arrival flow rate ($\frac{A_{LR/RL}}{S} = 1.4$), respectively. Also, the car occupancy is set as 1 for all test cases.

AM only considers adaptive main signal without pre-signals, which means the major structure of AMAP is reserved without constraint (7). FMFP refers to the fixed main signal with fixed pre-signal setting, and the set of pre-signals follow the traditional principles: If the main signal is red, then the pre-signal is red, otherwise, it changes to green [15]. FM only has fixed main signal without considering pre-signals. The setting of the fixed main signal is listed in Table III: As our method is developed based on a discrete-time model with time interval $\triangle = 10$s, the duration of each phase is also the integer times of $\triangle$. J_1, J_2 and J_3 refer to the intersections in Fig. 3 from left to right, respectively. The ratio of phases ϕ_1 and ϕ_2 for each intersection is determined by the critical lane volume, which can be found in [13]. Based on the above initial inputs, a half hour simulation is conducted under various car arrival rates, bus occupancies and bus headways.

Fig. 5, 6 and 7 illustrate the total passenger delay for cases 1 to 12 when car arrival flow is low, cases 13 to 24 when car arrival flow is medium and cases 25 to 36 when car arrival flow is high, respectively. Clearly, with the increase of the bus occupancy, the passenger delay increases accordingly, e.g., the delay comparison between case 1, case 2 and case 3. Also, a huge increase slope can be found when the bus frequency is high, and this is clearly shown in the increasing slope from case 1 to case 3, which is larger than the increasing trend between case 4 to case 6. And the largest passenger delay is obtained when the bus headway is 1 min,

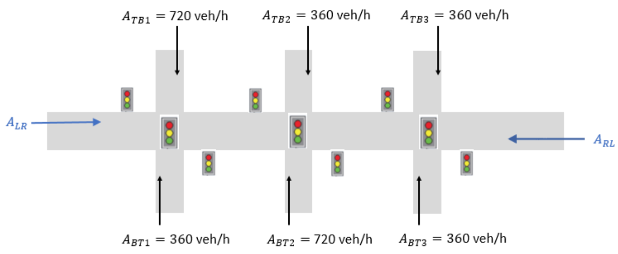

Fig. 3: Layout of the studied corridor

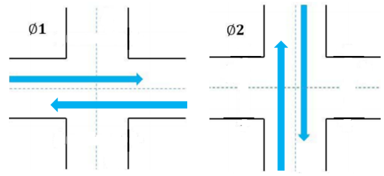

Fig. 4: Phase setting in the case study

TABLE I: The traffic volume inputs of the case studies

The ratio between the car arrival rate and the saturation flow rate	Saturation flow rate
$A_{LR}/S = 0.6, A_{RL}/S = 0.6$	$S = 1800$ veh/h
$A_{LR}/S = 1.0, A_{RL}/S = 1.0$	$S = 1800$ veh/h
$A_{LR}/S = 1.4, A_{RL}/S = 1.4$	$S = 1800$ veh/h

TABLE II: The case lists for Cases 1 to 12

	$\frac{A_{LR/RL}}{S}$ Ratio	Bus Occupancy	Bus Headway (min)
Case 1	0.6	30	1
Case 2	0.6	80	1
Case 3	0.6	160	1
Case 4	0.6	30	3
Case 5	0.6	80	3
Case 6	0.6	160	3
Case 7	0.6	30	6
Case 8	0.6	80	6
Case 9	0.6	160	6
Case 10	0.6	30	9
Case 11	0.6	80	9
Case 12	0.6	160	9

TABLE III: The main signal setting for the fixed-time strategy

	ϕ_1-J_1 (s)	ϕ_2-J_1 (s)	ϕ_1-J_2 (s)	ϕ_2-J_2 (s)	ϕ_1-J_3 (s)	ϕ_2-J_3 (s)	Cycle Time (s)	$\triangle$ (s)
Signal Setting for Cases 1-12	30	20	30	20	40	10	50	10
Signal Setting for Cases 13-24	40	20	40	20	50	10	60	10
Signal Setting for Cases 25-36	60	20	60	20	70	10	80	10

bus occupancy is 160 and the car arrival rate is high, namely, the yellow bar of case 27.

Moreover, the increase of the car arrival flow leads to the increase of the total passenger delay, which can be deduced by the increase of the range of the y axis from Fig. 5, Fig. 6 to Fig. 7. Also, all 36 cases indicate that AMAP outperforms the other three methods regardless of the bus headways, bus occupancies and car arrival rates. And the delay from AM method is smaller than FM for all cases, however, the comparison between its performance and FMFP depends on the bus occupancy and bus headway. For example, when the bus headway is large, especially for the cases when the headway becomes 9 min, AM outperforms FMFP no matter what the bus occupancy and the car arrival rate are. However, as the bus headway decreases to 6 min, the performance of AM and FMFP determined by the car arrival rate, which is clearly shown in case 9 and case 33 in Fig. 5 and Fig. 7, respectively. The advantage of FMFP reduces as the car arrival rate increases, this is understandable that the setting of the pre-signal definitely sacrifice the interest from private cars' side, and the large sacrifice due to the high arrival flow rates of private cars cannot be made up or exchange for the reduction of the bus total delay, which leads to the delay results shown in case 33. However, this phenomenon does not appear between FMFP and FM, and the FMFP outperforms FM in all cases. Also, the advantages of adding pre-signals become increasingly obvious with the increase of the bus frequency and bus occupancy.

In order to better illustrate the efficiency of the proposed method, the delay differences between AMAP and the other three methods under different car arrival rates are drawn in Fig. 8, Fig. 9 and Fig. 10, respectively. For three subgraphs shown in Fig 8/9/10, the upper left one indicates the delay difference between AMAP and AM, the upper right one refers to the delay difference between AMAP and FMFP, and the bottom one is the delay difference between AMAP and FM. The x-axis and y-axis of each subgraph represent the bus occupancy and the bus headway, respectively. The positive value of all bars reinforces the advantage of the proposed method.

For subgraphs in each Figure, the height of each bar increases with the increase of the bus occupancy and the decrease of the bus headway, which provides a large effects on the delay difference especially when the compared method does not consider the pre-signal setting, and this is clearly shown in the upper left subgraphs and the bottom subgraphs. However, the gap between AMAP and FMFP seems quite stable under different bus occupancies and bus headways. The above phenomena all indicate that the advantages of AMAP or the setting of pre-signals become more obvious when the bus services are frequent and the bus loading level is high.

On the other hand, by comparing the subgraphs under different car arrival rates, the gap of AMAP and other methods also increases as the car arrival rate increases, which can be found from the increase of the range of the y-axis. Although the range of the y-axis of the upper left subgraph and bottom graph in Fig. 10 does not change compared with Fig. 9, its actual values indeed increase as the car arrival flow ratio changes to 1.4, which is not reflected on the y-axis range. Therefore, this indicates that the advantages of AMAP become more obvious when the car arrival rate is high.

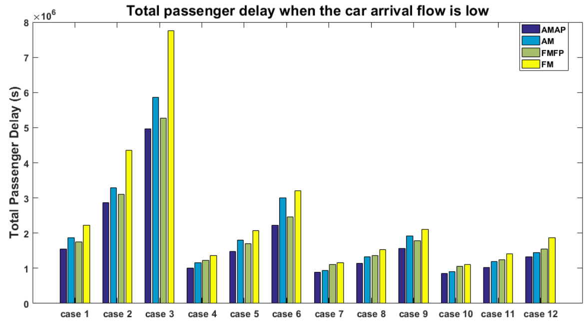

Fig. 5: Total passenger delay of four different methods under cases 1 to 12

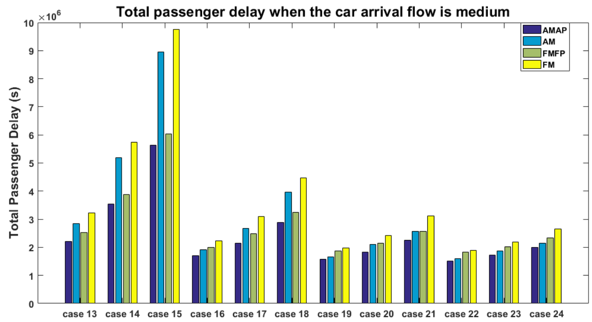

Fig. 6: Total passenger delay of four different methods under cases 13 to 24

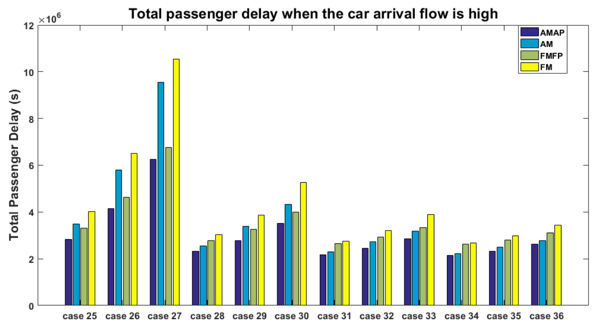

Fig. 7: Total passenger delay of four different methods under cases 25 to 36

IV. CONCLUSION

In this paper we have proposed an adaptive traffic signal strategy for the main signal as well as the pre-signal in order to minimize the passenger delay from the private cars and buses in the entire network. The link is partitioned into three different types of the cell: the car cell, the bus cell and the mixed cell. The states of the pre-signal and the main signal all become the decision variables in the

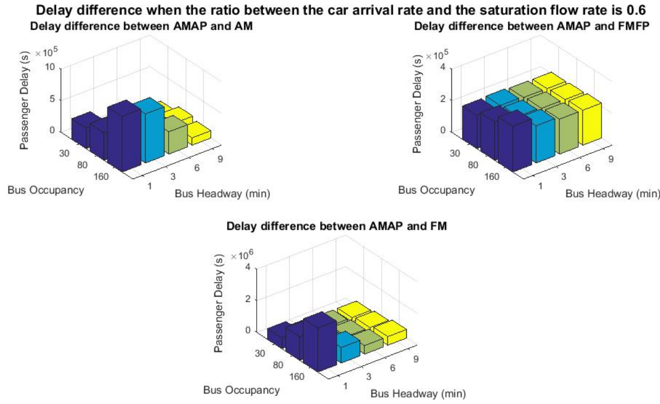

Fig. 8: Three delay difference graphs under the low car arrival rate by comparing the proposed method with the other three methods respectively

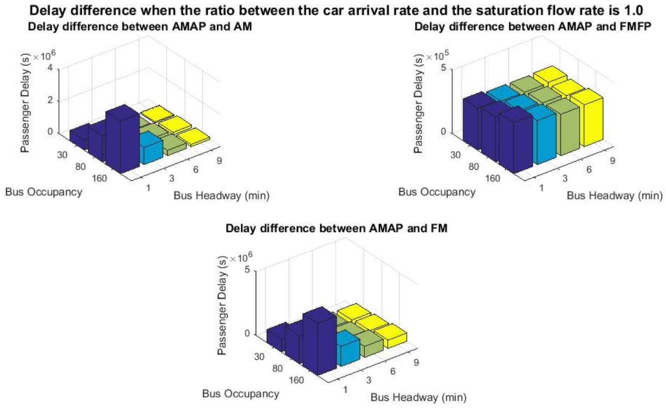

Fig. 9: Three delay difference graphs under the medium car arrival rate by comparing the proposed method with the other three methods respectively

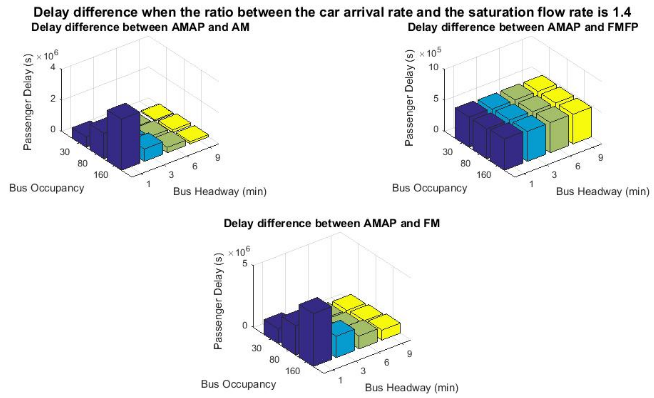

Fig. 10: Three delay difference graphs under the high car arrival rate by comparing the proposed method with the other three methods respectively

model, which is determined based on the objective, namely, the total passenger delay is minimized. To overcome the tedious transformation process and the high computational complexity in traditional MILP problems, the HS algorithm is adopted to solve the optimization model in real time. The results of the case studies indicate that the proposed AMAP strategy outperforms the other three strategies under various traffic compositions, and the necessity to set pre-signal becomes obvious when the bus occupancy and the bus frequency are high. Moreover, in order to make the simulation more realistic, multiple phases involving turning flows and the connection with VISSIM should be considered in our future work.

REFERENCES

[1] Michael Eichler and Carlos F Daganzo. Bus lanes with intermittent priority: Strategy formulae and an evaluation. *Transportation Research Part B: Methodological*, 40(9):731–744, 2006.

[2] S Ilgin Guler and Monica Menendez. Analytical formulation and empirical evaluation of pre-signals for bus priority. *Transportation Research Part B: Methodological*, 64:41–53, 2014.

[3] S Ilgin Guler and Monica Menendez. Evaluation of presignals at oversaturated signalized intersections. *Transportation research record*, 2418(1):11–19, 2014.

[4] S Ilgin Guler and Monica Menendez. Pre-signals for bus priority: basic guidelines for implementation. *Public Transport*, 7(3):339–354, 2015.

[5] Haitao He, Ilgin S Guler, and Monica Menendez. The effects of pre-signals at an isolated intersection: simulation results. In *14th Swiss Transport Research Conference (STRC 2014)*. Swiss Transport Research Conference (STRC), 2014.

[6] Haitao He, S Ilgin Guler, and Monica Menendez. Adaptive control algorithm to provide bus priority with a pre-signal. *Transportation Research Part C: Emerging Technologies*, 64:28–44, 2016.

[7] Qing He, K Larry Head, and Jun Ding. Multi-modal traffic signal control with priority, signal actuation and coordination. *Transportation Research Part C: Emerging Technologies*, 46:65–82, 2014.

[8] Jia Hu, Byungkyu Brian Park, and Young-Jae Lee. Coordinated transit signal priority supporting transit progression under connected vehicle technology. *Transportation Research Part C: Emerging Technologies*, 55:393–408, 2015.

[9] Jia Hu, Byungkyu Brian Park, and Young-Jae Lee. Transit signal priority accommodating conflicting requests under connected vehicles technology. *Transportation Research Part C: Emerging Technologies*, 69:173–192, 2016.

[10] Miran Khwais and Jack Haddad. Optimal pre-signal control for buses and cars at isolated signalized intersections. *IFAC-PapersOnLine*, 50(1):9706–9711, 2017.

[11] Yiching Lin, Xianfeng Yang, Nan Zou, and Mark Franz. Transit signal priority control at signalized intersections: a comprehensive review. *Transportation letters*, 7(3):168–180, 2015.

[12] Wanjing Ma, Wei Ni, Larry Head, and Jing Zhao. Effective coordinated optimization model for transit priority control under arterial progression. *Transportation Research Record*, 2366(1):71–83, 2013.

[13] Roger P Roess, Elena S Prassas, and William R McShane. *Traffic engineering*. Pearson/Prentice Hall, 2004.

[14] José Viegas and Baichuan Lu. The intermittent bus lane signals setting within an area. *Transportation Research Part C: Emerging Technologies*, 12(6):453–469, 2004.

[15] Jianping Wu and Nick Hounsell. Bus priority using pre-signals. *Transportation Research Part A: Policy and Practice*, 32(8):563–583, 1998.

[16] Yiguang Xuan, Carlos F Daganzo, and Michael J Cassidy. Increasing the capacity of signalized intersections with separate left turn phases. *Transportation research part B: Methodological*, 45(5):769–781, 2011.

[17] Yi Zhang, Kaizhou Gao, Yicheng Zhang, and Rong Su. Traffic light scheduling for pedestrian-vehicle mixed-flow networks. *IEEE Transactions on Intelligent Transportation Systems*, 20(4):1468–1483, 2018.

[18] Yi Zhang, Yicheng Zhang, and Rong Su. Optimization of vehicle delay and drivers' unhappiness at a signalized network: a multi-objective approach. In *2019 IEEE 15th International Conference on Control and Automation (ICCA)*, pages 622–627. IEEE, 2019.

[19] Yi Zhang, Yicheng Zhang, and Rong Su. Pedestrian-safety-aware traffic light control strategy for urban traffic congestion alleviation. *IEEE Transactions on Intelligent Transportation Systems*, 2019. Early Access, Doi = 10.1109/TITS.2019.2955752.